# Order-$\alpha_s$ calculation of hadronic $W^-W^+$ production

J. Ohnemus
*Department of Physics, Florida State University, Tallahassee, Florida 32306*
(Received 26 March 1991)

An order-$\alpha_s$ calculation of $p\overset{(-)}{p} \to W^-W^+ + X$ is presented. Results are given for the total cross section and differential distributions for Fermilab Tevatron, CERN Large Hadron Collider, and Superconducting Super Collider energies. The calculation utilizes a combination of analytic and Monte Carlo integration methods which makes it easy to calculate a variety of observables and to impose experimental cuts.

## I. INTRODUCTION

The production of $W^-W^+$ pairs at hadron supercolliders will be an important process for testing the standard model [1]. If the Higgs boson is heavier than twice the $Z$-boson mass, it will decay almost exclusively into $W$- or $Z$-boson pairs [2]. The existence of the Higgs boson would then be signaled by a peak in the invariant-mass distribution of the weak-boson pair. Charged-weak-boson pairs can also be used to study the trilinear coupling of weak gauge bosons [3]. The production of $W$ pairs could also signal new physics since new heavy particles often decay into weak-boson pairs, for example, heavy squarks and gluinos can decay into $W^-W^+$. In order to perform these tests it is important to have a precise calculation of continuum $W^-W^+$ production.

The main source of continuum $W^-W^+$ production is $q\bar{q}$ annihilation which proceeds via $t$-channel quark exchange and $s$-channel $Z$-boson and photon exchange [4]. Other sources of continuum $W^-W^+$ production, in order of their importance, are gluon fusion, $W^-W^+$ fusion, and $ZZ$ fusion. The cross section for $W^-W^+$ production from gluon fusion via a quark box loop is 20–25 % as big as the lowest-order $q\bar{q}$-annihilation cross section [5]. Gluon fusion can also proceed via a triangle heavy-quark loop with Higgs-boson exchange in the $s$-channel [6] ($gg \to H \to W^-W^+$). This process is mainly of interest as a source of Higgs bosons; away from the Higgs resonance this cross section is only a small fraction of the $q\bar{q}$-annihilation cross section. In the weak-boson fusion processes [7] the incoming quarks radiate two vector bosons which subsequently scatter off each other. These processes are again mainly of interest as sources of Higgs bosons, with the Higgs boson appearing as an $s$-channel resonance; away from the Higgs resonance, the weak-boson fusion cross sections are only a small fraction of the $q\bar{q}$-annihilation cross section. The cross section for the $W^-W^+$ fusion process, $pp \to W^-W^+ \to W^-W^+$, is about an order of magnitude smaller than the $q\bar{q}$-annihilation cross section, while the cross section for the $ZZ$ fusion process, $pp \to ZZ \to W^-W^+$, is about half as large as the $W^-W^+$ fusion cross section. Pair production of $W^-W^+$ bosons in association with jets has also been calculated [8, 9].

Until now $W^-W^+$ production has been calculated only in the leading-logarithm approximation and the order-$\alpha_s$ corrections have only been estimated [10] using the soft-gluon approximation [11]. A complete next-to-leading-logarithm (NLL) calculation of hadronic $W^-W^+$ production is presented in this paper. At the parton level this involves computing the contributions from the $2 \to 3$ real emission processes $q\bar{q} \to W^-W^+g$, $qg \to W^-W^+q$, and $\bar{q}g \to W^-W^+\bar{q}$ as well as the one-loop corrections to the $2 \to 2$ process $q\bar{q} \to W^-W^+$. The focus of the present calculation is on the order-$\alpha_s$ corrections to $W^-W^+$ production. Accordingly, the order-$\alpha_s^2$ gluon fusion contribution has not been included. However, this contribution should eventually be included when calculating the full $W^-W^+$ continuum background since it can be significant at supercollider energies.

The NLL calculation presented here makes use of a combination of analytic and Monte Carlo integration methods. The methods used here are the same as those used in Ref. [12] for the NLL calculation of hadronic $ZZ$ production. Similar methods have also been used to perform NLL calculations for direct photon production [13], photoproduction [14], symmetric dihadron production [15], and $W$ production [16]. The Monte Carlo approach to NLL calculations has many advantages over a purely analytic calculation. The Monte Carlo approach allows one to calculate any number of observables simultaneously by simply histogramming the appropriate quantities. Futhermore, it is easy to tailor the Monte Carlo calculation to different experimental conditions, for example, detector acceptances, experimental cuts, and jet definitions. Also, with the Monte Carlo approach one can easily study the NLL corrections for different observables, the variation of the NLL corrections in different regions of phase space, and the dependence of the NLL cross section on the choice of scale.

The procedure for the NLL $W^-W^+$ calculation is identical to the procedure used in Ref. [12] for the NLL $ZZ$ calculation. In fact, most of the expressions for the $W^-W^+$ case can be obtained from the corresponding expressions for the $ZZ$ case by simply replacing the $ZZ$ Born cross section with the $W^-W^+$ Born cross section. The only exception to this rule is the finite virtual cor-

 

rection, which must be calculated anew. Thus only the final expressions for the NLL $W^-W^+$ calculation will be given in this paper. Details on the derivations of these expressions can be found in Ref. [12].

The remainder of this paper is organized as follows. Section II describes the techniques used in the Monte Carlo approach to NLL calculations. The NLL calculation of $W^-W^+$ production is described in Sec. III. Results are presented in Sec. IV and summary remarks are given in Sec. V. Finally, there are three appendices containing details of the regularization of $\gamma_5$ and lengthy expressions from the calculation.

## II. MONTE CARLO FORMALISM

The Monte Carlo formalism for NLL calculations has been described in detail in Refs. [12–16] so the discussion here will be brief. The basic challenge is to design a program which retains the versatility inherent in a Monte Carlo approach while ensuring that all of the required cancelations of singularities still takes place. In order to discuss the technique for isolating the various singularities, let the four-vectors of the two-body and three-body subprocesses be labeled by $p_1+p_2 \to p_3+p_4$ and $p_1+p_2 \to p_3+p_4+p_5$, respectively, and define the Lorentz scalars $s_{ij}=(p_i+p_j)^2$ and $t_{ij}=(p_i-p_j)^2$. The $W^-W^+$ calculation contains infrared (IR) and collinear singularities but no ultraviolet singularities. Dimensional regularization [17] is used to isolate the singularities. First, three-body phase space is partitioned into singular and finite regions by introducing soft and collinear cutoff parameters $\delta_s$ and $\delta_c$. The soft region of phase space is defined to be the region where the gluon energy in the subprocess rest frame becomes less than $\delta_s\sqrt{s_{12}}/2$. The collinear regions of phase space are defined to be those regions where any invariant ($s_{ij}$ or $t_{ij}$) becomes smaller in magnitude than $\delta_c s_{12}$. Next, the squared three-body matrix elements are approximated in the singular regions; the soft gluon and leading-pole approximations are used in the soft and collinear regions, respectively. The resulting expressions are then integrated over the singular regions of phase space. At this stage the integrated expressions contain finite two-body contributions as well as singular pieces. The singularities from the soft region will cancel the virtual IR singularities while the singularities from the collinear region will be factorized into the parton distribution function. The remainder of three-body phase space contains no singularities and the subprocesses can be evaluated in four dimensions.

The calculation now consists of two pieces — a set of two-body contributions and a set of three-body contributions. Each set consists of finite parts, all singularities having been canceled or factorized. At this stage both pieces depend on the values chosen for the two theoretical cutoffs $\delta_s$ and $\delta_c$ so that each piece by itself has no intrinsic meaning. However, when the two- and three-body contributions are combined to form a suitably inclusive observable all dependence on the cutoffs cancels. The cutoffs merely serve to distinguish the regions where the phase space integrations are done by hand from those where they are done by Monte Carlo simulation. When the results are added together, the precise location of the boundary between the two regions is not relevant. The results reported below are stable to reasonable variations in the cutoffs, thus providing a check on the calculation.

## III. NEXT-TO-LEADING-LOGARITHM FORMALISM

### A. Born process

The Feynman diagrams that contribute to the Born amplitude for the reaction

$$q(p_1)+\bar{q}(p_2) \longrightarrow W^-(p_3)+W^+(p_4) \tag{1}$$

are shown in Fig. 1. The Born amplitude in $N$ dimensions is

$$\mathcal{M}^{\rm Born} = \delta_{i_1 i_2}\, e^2\, \mu^{4-N}\, \epsilon_\mu^*(p_3)\, \epsilon_\nu^*(p_4) \times \sum_{\tau=\pm} \bar{V}(p_2) P_{-\tau} T^{\mu\nu} U(p_1)\,, \tag{2}$$

where $\delta_{i_1 i_2}$ is the color tensor ($i_1, i_2$ are color indices for quarks 1 and 2), $e$ is the electromagnetic coupling constant, $\mu$ is a mass parameter introduced to keep the couplings dimensionless, $\epsilon_\mu^*(p_3)$ and $\epsilon_\nu^*(p_4)$ are the $W$-boson polarization tensors, and $P_\tau$ denotes the left-right-projection operator $P_\tau = \frac{1}{2}(1+\tau\gamma_5)$. The tensor $T^{\mu\nu}$ is

$$T^{\mu\nu} = \theta(Q_q)\left(g_\tau^{qWq'}\right)^2 \gamma^\mu \frac{\not p_1 - \not p_4}{u}\gamma^\nu + \theta(-Q_q)\left(g_\tau^{qWq'}\right)^2 \gamma^\nu \frac{\not p_1 - \not p_3}{t}\gamma^\mu - \left(\frac{1}{s}\, g_\tau^{q\gamma q} + \frac{\cot\theta_W}{s - M_Z^2 + i\Gamma_Z M_Z}\, g_\tau^{qZq}\right)\left[(\not p_3 - \not p_4) g^{\mu\nu} + (2p_4+p_3)^\mu \gamma^\nu - (2p_3+p_4)^\nu \gamma^\mu\right], \tag{3}$$

where $\theta(x)$ is the step function. The right- and left-handed weak-boson-to-quark couplings are denoted by $g_\pm^{qVq}$:

$$g_-^{uWd} = g_-^{dWu} = \frac{1}{\sqrt{2}\sin\theta_W}\,, \quad g_+^{uWd} = g_+^{dWu} = 0\,,$$

$$g_-^{qZq} = \frac{T_3^q}{\sin\theta_W\cos\theta_W} - Q_q\tan\theta_W\,,$$

$$g_+^{qZq} = -Q_q\tan\theta_W\,, \tag{4}$$

$$g_-^{q\gamma q} = Q_q\,, \quad g_+^{q\gamma q} = Q_q\,,$$

where $Q_q$ and $T_3^q$ denote the electric charge (in units of the proton charge $e$) and the third component of weak isospin of quark $q$, and $\theta_W$ is the weak mixing angle. The kinematic invariants $s, t, u$ are defined by

$$s=(p_1+p_2)^2\,,\quad t=(p_1-p_3)^2\,,\quad u=(p_1-p_4)^2\,. \tag{5}$$

The squared amplitude summed over final-state polarizations and initial state spins can be written

$$|\mathcal{M}^{\rm Born}|^2 = N_C\, e^4\, \mu^{4\epsilon}(A_1^q B_1^q + A_2^q B_2^q + A_3^q B_3^q), \tag{6}$$

where $N_C$ is the number of colors, $A_i^q$ contains coupling and propagator factors, $B_i^q$ are functions of the kinematic invariants, and the number of space-time dimensions is $N=4-2\epsilon$. For up-type quarks the $A_i^q$ factors are

$$\begin{aligned}
A_1^u &= \frac{1}{2}\left(g_-^{uWd}\right)^4\,,\\
A_2^u &= \frac{1}{2}\left[\left(g_-^{u\gamma u}\right)^2+\left(g_+^{u\gamma u}\right)^2\right]+\frac{1}{2}\frac{s^2}{(s-M_Z^2)^2+(\Gamma_Z M_Z)^2}\left[\left(g_-^{uZu}\right)^2+\left(g_+^{uZu}\right)^2\right]\cot^2\theta_W\\
&\quad+\frac{s(s-M_Z^2)}{(s-M_Z^2)^2+(\Gamma_Z M_Z)^2}\left(g_-^{u\gamma u}g_-^{uZu}+g_+^{u\gamma u}g_+^{uZu}\right)\cot\theta_W\,,\\
A_3^u &= -\left(g_-^{uWd}\right)^2\left(g_-^{u\gamma u}+\frac{s(s-M_Z^2)}{(s-M_Z^2)^2+(\Gamma_Z M_Z)^2}\,g_-^{uZu}\cot\theta_W\right).
\end{aligned} \tag{7}$$

The $A_i^d$ factors for down-type quarks are obtained by interchanging $u\leftrightarrow d$ in the $A_i^u$ factors. The $B_i^q$ expressions for up-type quarks are

$$\begin{aligned}
B_1^u &= \left(\frac{2tu}{M_W^4}-\frac{8M_W^4}{u^2}-\frac{8(t+u)}{M_W^2}+\frac{8t}{u}+14\right)+\epsilon\left(\frac{8(t+u)}{M_W^2}-\frac{16(t+u)}{u}+\frac{16M_W^4}{u^2}\right)+\epsilon^2\left(\frac{8t}{u}-\frac{8M_W^4}{u^2}\right),\\
B_2^u &= \left(\frac{2tu(t+u)^2}{M_Z^4s^2}-\frac{8(t^3+u^3)}{M_Z^2s^2}-\frac{24tu(t+u)}{M_Z^2s^2}+\frac{32(t+u)M_Z^2}{s^2}+\frac{14(t^2+u^2)}{s^2}+\frac{44tu}{s^2}-\frac{80M_Z^4}{s^2}\right)\\
&\quad+\epsilon\left(\frac{8(t^3+u^3)}{M_Z^2s^2}+\frac{24tu(t+u)}{M_Z^2s^2}-\frac{32(t+u)M_Z^2}{s^2}-\frac{16(t^2+u^2)}{s^2}+\frac{80M_Z^4}{s^2}-\frac{48tu}{s^2}\right),\\
B_3^u &= \left(-\frac{2tu(t+u)}{M_Z^4s}+\frac{8(t+u)^2}{M_Z^2s}-\frac{22t}{u}-\frac{14u}{s}-\frac{16(t+u)M_Z^2}{su}+\frac{40M_Z^4}{su}\right)\\
&\quad+\epsilon\left(-\frac{8(t+u)^2}{M_Z^2s}+\frac{16(t+u)M_Z^2}{su}+\frac{24t}{s}+\frac{16u}{s}-\frac{40M_Z^4}{su}\right).
\end{aligned} \tag{8}$$

The $B_i^q$ expressions for down-type quarks are related to the $B_i^q$ expressions for up-type quarks by the relations

$$\begin{aligned}
B_1^d &= B_1^u(t\leftrightarrow u)\,,\\
B_2^d &= B_2^u\,,\\
B_3^d &= -B_3^u(t\leftrightarrow u)\,.
\end{aligned} \tag{9}$$

The details for treating $\gamma_5$ in $N$ dimensions are described in Appendix A. The algebra for this paper was evaluated using the computer algebra program FORM [18].

The Born subprocess cross section is

$$d\hat\sigma^{\rm Born}(q\bar q\to W^-W^+) = \frac{1}{4}\frac{1}{9}\frac{1}{2s}\,|\mathcal{M}^{\rm Born}|^2\,d^N\Phi_2, \tag{10}$$

where the factors $\frac{1}{4}$ and $\frac{1}{9}$ are the spin average and color average, respectively, and the two-body phase space is

$$d^N\Phi_2 = \frac{1}{8\pi}\left(\frac{4\pi}{s}\right)^{\epsilon}\frac{1}{\Gamma(1-\epsilon)}\left(1-\frac{4M_W^2}{s}\right)^{1/2-\epsilon} \times v^{-\epsilon}(1-v)^{-\epsilon}\,dv\,, \tag{11}$$

with $v=\frac{1}{2}(1+\cos\theta)$. It is convenient to decompose the squared Born amplitude into three terms corresponding to the power of $\epsilon$ that appears in the squared amplitude

$$|\mathcal{M}^{\rm Born}|^2 = |\mathcal{M}_0^{\rm Born}|^2+\epsilon|\mathcal{M}_1^{\rm Born}|^2+\epsilon^2|\mathcal{M}_2^{\rm Born}|^2\,, \tag{12}$$

with this decomposition the Born cross section can be written

$$d\hat\sigma^{\rm Born} = d\hat\sigma_0^{\rm Born}+\epsilon\,d\hat\sigma_1^{\rm Born}+\epsilon^2 d\hat\sigma_2^{\rm Born}\,. \tag{13}$$

This decomposition will be useful later for writing the virtual and soft corrections.

The leading-logarithm (LL) cross section is obtained by convoluting the subprocess cross section with the parton densities and summing over the contributing partons:

$$\begin{aligned}
\sigma^{\rm LL}(pp\to W^-W^+) &= \sum_q\int d\,\hat\sigma^{\rm Born}(q\bar q\to W^-W^+)\\
&\quad\times\left[G_{q/p}(x_1,M^2)G_{\bar q/p}(x_2,M^2)+x_1\leftrightarrow x_2\right]dx_1dx_2\,.
\end{aligned} \tag{14}$$

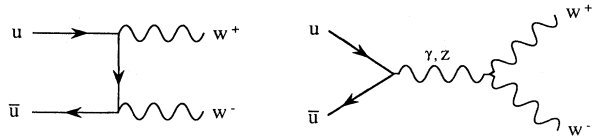


FIG. 1. Feynman diagrams for the Born subprocess $u\bar{u} \to W^-W^+$. The straight and wavy lines denote quarks and electroweak bosons, respectively. The diagrams for the subprocess $d\bar{d} \to W^-W^+$ are obtained by replacing $u \to d$ and $W^- \leftrightarrow W^+$ in the diagrams shown here.

### B. Virtual processes

The order-$\alpha_s$ virtual correction to $q\bar{q} \to W^-W^+$ comes from the interference between the Born graphs of Fig. 1 and the virtual graphs shown in Fig. 2. The interference between these amplitudes has been evaluated in $N$ dimensions using the Feynman parametrization technique. There are two mitigating factors which simplify the $q\bar{q} \to W^-W^+$ virtual calculation. The first is that the calculation does not contain UV singularities since the graphs in Fig. 2 do not contribute to the renormalization of the strong-, electromagnetic-, or weak-coupling constants. The second is that the self-energy insertions on the external quark lines vanish because of the cancelation of the UV and IR divergences [19]. Basically, what happens is that the UV and IR poles cancel when one does not distinguish between them.

Because the loop integrals associated with the four-point function from the box diagrams in Fig. 2 are very difficult to evaluate when powers of the loop momenta appear in the numerator, it is advantageous to first multiply the Born amplitudes times the virtual amplitudes and evaluate the resulting traces. The numerator of the resulting expression can then be rewritten, using momentum conservation relations, such that propagator denominator factors cancel with identical factors in the numerator. This way the four-point functions with powers of the loop momentum in the numerator are reduced to a four-point function with a constant numerator and three- and two-point functions which are easier to evaluate. The loop integrals can be reduced to a set of 12 integrals. The first 11 of these integrals were given in Ref. [12] and the twelfth integral is given in Appendix B.

The order-$\alpha_s$ virtual contribution to the $q\bar{q} \to W^-W^+$ cross section is

$$\frac{d\hat{\sigma}^{\rm virt}}{dv} = C_F \frac{\alpha_s}{2\pi} \left(\frac{4\pi\mu^2}{s}\right)^{\epsilon} \frac{\Gamma(1-\epsilon)}{\Gamma(1-2\epsilon)} \times \left( -\frac{2}{\epsilon^2}\frac{d\hat{\sigma}_0^{\rm Born}}{dv} - \frac{2}{\epsilon}\frac{d\hat{\sigma}_1^{\rm Born}}{dv} - \frac{3}{\epsilon}\frac{d\hat{\sigma}_0^{\rm Born}}{dv} + \frac{1}{4}\frac{1}{9} N_C\, e^4\, F^{\rm virt}(s,t,u,M_W^2) \right), \quad (15)$$

where $d\hat{\sigma}_0^{\rm Born}$ and $d\hat{\sigma}_1^{\rm Born}$ are defined by Eq. (13) and $C_F = \frac{4}{3}$ is the quark-gluon vertex color factor. The order-$\alpha_s$ finite virtual correction is contained in the function $F^{\rm virt}(s,t,u,M_W^2)$ which is given in Appendix C.

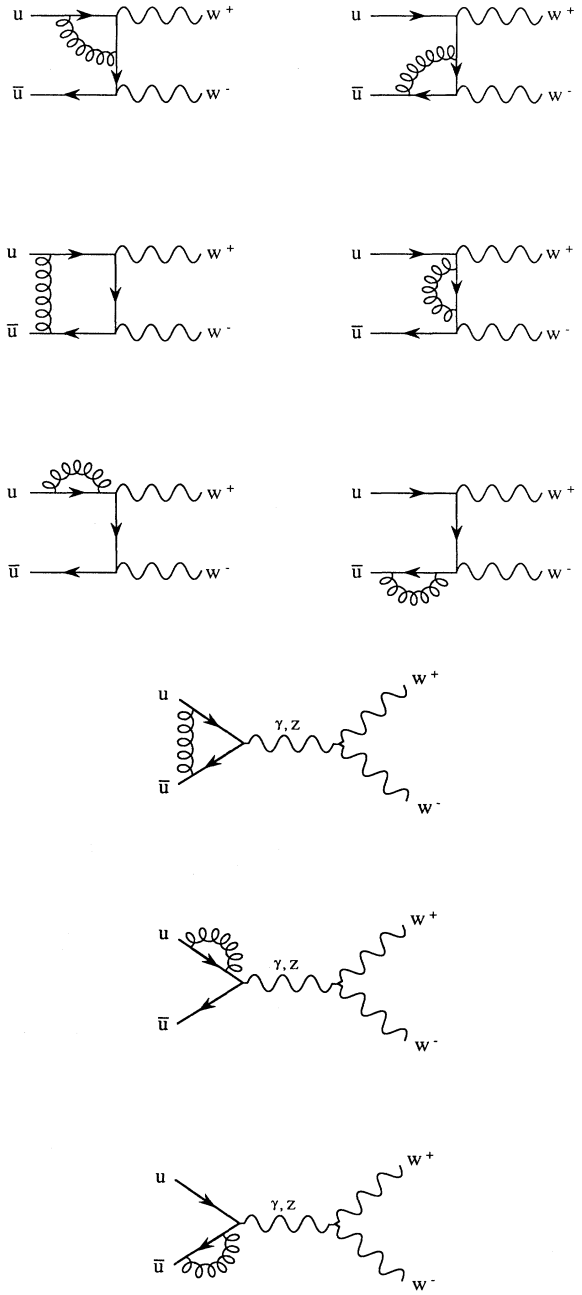


FIG. 2. Feynman diagrams for the virtual subprocess $u\bar{u} \to W^-W^+$. The straight, wavy, and curly lines denote quarks, electroweak bosons, and gluons, respectively. The diagrams for the subprocess $d\bar{d} \to W^-W^+$ are obtained by replacing $u \to d$ and $W^- \leftrightarrow W^+$ in the diagrams shown here.

### C. Soft-gluon emission

The Feynman diagrams for the real emission subprocess

$$q(p_1) + \bar{q}(p_2) \longrightarrow W^-(p_3) + W^+(p_4) + g(p_5) \quad (16)$$

are shown in Fig. 3. In the soft-gluon region of three-body phase space, which is defined by $E_5 < \delta_s \sqrt{s_{12}}/2$, the soft-gluon contribution to the cross section is

$$\frac{d\hat{\sigma}^{\rm soft}}{dv} = C_F \frac{\alpha_s}{2\pi}\left(\frac{4\pi\mu^2}{s}\right)^{\epsilon}\frac{\Gamma(1-\epsilon)}{\Gamma(1-2\epsilon)}\left[\frac{2}{\epsilon^2}\frac{d\hat{\sigma}_0^{\rm Born}}{dv} + \frac{2}{\epsilon}\left(-2\ln(\delta_s)\frac{d\hat{\sigma}_0^{\rm Born}}{dv} + \frac{d\hat{\sigma}_1^{\rm Born}}{dv}\right)\right.$$
$$\left. +4\ln(\delta_s)^2\frac{d\hat{\sigma}_0^{\rm Born}}{dv} - 4\ln(\delta_s)\frac{d\hat{\sigma}_1^{\rm Born}}{dv} + 2\frac{d\hat{\sigma}_2^{\rm Born}}{dv}\right], \tag{17}$$

where $\delta_s$ is the soft cutoff parameter defined in Sec. II.

### D. Hard collinear corrections

The $2 \to 3$ real emission processes have hard collinear singularities when $t_{15} \to 0$ or $t_{25} \to 0$. These singularities must be factorized and absorbed into the initial-state parton distributions. The collinear regions of three-body phase space are defined to be those regions where any invariant ($s_{ij}$ or $t_{ij}$) becomes smaller in magnitude than $\delta_c s_{12}$, where $\delta_c$ is the collinear cutoff parameter defined in Sec. II. After the factorization is performed, the remnants of the hard collinear singularities take the form

$$\frac{d\tilde{\sigma}}{dv}(q\bar{q} \to W^-W^+) = \frac{\alpha_s}{2\pi}\frac{d\hat{\sigma}_0^{\rm Born}}{dv}\left\{ G_{q/p}(x_1,M^2)\int_{x_2}^{1-\delta_s}\frac{dz}{z}\left[G_{\bar{q}/p}\left(\frac{x_2}{z},M^2\right)\tilde{P}_{qq}(z) + G_{g/p}\left(\frac{x_2}{z},M^2\right)\tilde{P}_{qg}(z)\right]\right.$$
$$\left. + G_{\bar{q}/p}(x_2,M^2)\int_{x_1}^{1-\delta_s}\frac{dz}{z}\left[G_{q/p}\left(\frac{x_1}{z},M^2\right)\tilde{P}_{qq}(z) + G_{g/p}\left(\frac{x_1}{z},M^2\right)\tilde{P}_{qg}(z)\right]\right\}, \tag{18}$$

with

$$\tilde{P}_{ij}(z) \equiv P_{ij}(z)\ln\left(\frac{1-z}{z}\delta_c\frac{s}{M^2}\right) - P'_{ij}(z) - \lambda F_{ij}(z). \tag{19}$$

The Altarelli-Parisi splitting functions in $N = 4 - 2\epsilon$ dimensions for $0 < z < 1$ are

$$P_{qq}(z,\epsilon) = C_F\left(\frac{1+z^2}{1-z} - \epsilon(1-z)\right),$$
$$P_{qg}(z,\epsilon) = \frac{1}{2(1-\epsilon)}\left[z^2 + (1-z)^2 - \epsilon\right], \tag{20}$$

and can be written

$$P_{ij}(z,\epsilon) = P_{ij}(z) + \epsilon P'_{ij}(z), \tag{21}$$

which defines the $P'_{ij}$ functions. The functions $F_{qq}$ and $F_{qg}$ depend on the choice of factorization convention and the parameter $\lambda$ specifies the factorization convention; $\lambda = 0$ for the universal [modified minimal subtraction ($\overline{\rm MS}$)] convention and $\lambda = 1$ for the physical [deep-inelastic scattering (DIS)] convention. For the physical convention the factorization functions are

$$F_{qq}(z) = C_F\left[\frac{1+z^2}{1-z}\ln\left(\frac{1-z}{z}\right) - \frac{3}{2}\frac{1}{1-z} + 2z + 3\right], \tag{22}$$

$$F_{qg}(z) = \frac{1}{2}\left[[z^2 + (1-z)^2]\ln\left(\frac{1-z}{z}\right) + 8z(1-z) - 1\right].$$

The parameter $M^2$ is the factorization scale which must be specified in the process of factorizing the collinear singularity. Basically, it determines how much of the collinear term is absorbed into the various parton distributions.

The upper limit on the integrals appearing in Eq. (18) is determined by requiring that the hard collinear term not overlap with the soft region previously discussed. If such an overlap were to occur, then that region of three-body phase space would be counted twice.

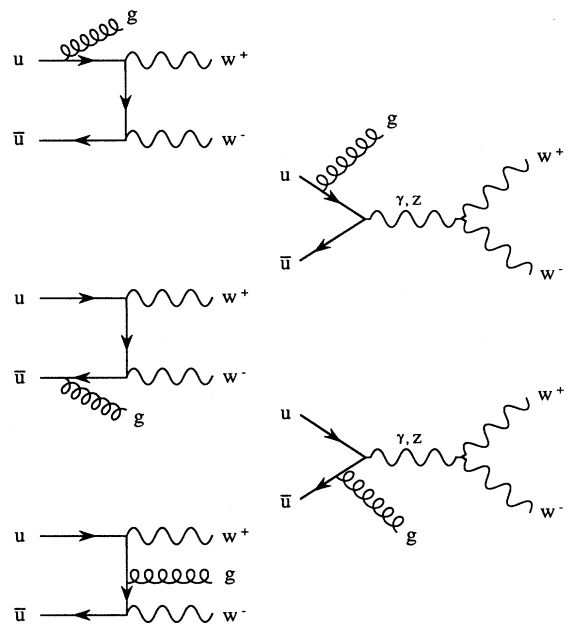


FIG. 3. Feynman diagrams for the real emission subprocess $u\bar{u} \to W^-W^+g$. The straight, wavy, and curly lines denote quarks, electroweak bosons, and gluons, respectively. The diagrams for the subprocess $d\bar{d} \to W^-W^+g$ are obtained by replacing $u \to d$ and $W^- \leftrightarrow W^+$ in the diagrams shown here.

### E. Soft collinear subtraction term

The $M^2$-dependent subtraction piece which is used to absorb the collinear singularity into the parton distribution functions involves an integral over splitting functions with the upper limit corresponding to $z = 1$, not $1 - \delta_s$. Therefore, there is one last piece to be subtracted which, for the $t_{15}$ case, takes the form

$$\frac{d\hat{\sigma}^{15}}{dv} = \frac{d\hat{\sigma}^{\rm Born}}{dv}\frac{\alpha_s}{2\pi}\left(\frac{4\pi\mu^2}{M^2}\right)^{\epsilon}\frac{\Gamma(1-\epsilon)}{\Gamma(1-2\epsilon)} \times \int_{1-\delta_s}^{1}\frac{dz}{z}\left(-\frac{1}{\epsilon}P_{qq}(z) + \lambda F_{qq}(z)\right) G_{q/p}(x/z)\,. \tag{23}$$

Inserting $P_{qq}$ and $F_{qq}$ and integrating yields

$$\begin{aligned}\frac{d\hat{\sigma}^{15}}{dv} = -C_F\frac{\alpha_s}{2\pi}\left(\frac{4\pi\mu^2}{s}\right)^{\epsilon}\frac{\Gamma(1-\epsilon)}{\Gamma(1-2\epsilon)}\Bigg[ &\frac{1}{\epsilon}\left(\frac{3}{2}+2\ln(\delta_s)\right)\frac{d\hat{\sigma}_0^{\rm Born}}{dv} \\ &+\left(\frac{3}{2}+2\ln(\delta_s)\right)\left[\ln\left(\frac{s}{M^2}\right)\frac{d\hat{\sigma}_0^{\rm Born}}{dv}+\frac{d\hat{\sigma}_1^{\rm Born}}{dv}\right] \\ &+\lambda\left(\frac{9}{2}+\frac{\pi^2}{3}+\frac{3}{2}\ln(\delta_s)-\ln(\delta_s)^2\right)\frac{d\hat{\sigma}_0^{\rm Born}}{dv}\Bigg]\,,\end{aligned} \tag{24}$$

where terms proportional to a power of the soft cutoff $\delta_s$ have been discarded. The soft collinear singularity in the $t_{25} \to 0$ region yields an identical result.

### F. Next-to-leading-logarithm cross section

The NLL cross section, which consists of two- and three-body contributions, can now be assembled from the pieces described in the previous sections. The two-body contribution is

$$\sigma_{\rm 2body}^{\rm NLL}(pp \to W^-W^+) = \sum_q \int dv\, dx_1\, dx_2 \left( G_{q/p}(x_1, M^2)\, G_{\bar{q}/p}(x_2, M^2)\frac{d\hat{\sigma}^{\rm NLL}}{dv}(q\bar{q} \to W^-W^+) + (x_1 \leftrightarrow x_2) + \frac{d\tilde{\sigma}}{dv}\right)\,, \tag{25}$$

where the sum is over all contributing quark flavors, $d\tilde{\sigma}/dv$ is defined in Eq. (18) and

$$\frac{d\hat{\sigma}^{\rm NLL}}{dv}(q\bar{q} \to W^-W^+) = \frac{d\hat{\sigma}^{\rm Born}}{dv} + \frac{d\hat{\sigma}^{\rm virt}}{dv} + \frac{d\hat{\sigma}^{\rm soft}}{dv} - \frac{d\hat{\sigma}^{15}}{dv} - \frac{d\hat{\sigma}^{25}}{dv}\,. \tag{26}$$

The $1/\epsilon^2$ and $1/\epsilon$ poles cancel when the terms in Eq. (26) are summed [see Eqs. (10), (15), (17), and (24)].

The three-body contribution to the cross section is

$$\sigma_{\rm 3body}(pp \to W^-W^+ + X) = \sum_{abc}\int d\hat{\sigma}(ab \to W^-W^+c)\left[G_{a/p}(x_1, M^2)\, G_{b/p}(x_2, M^2) + (x_1 \leftrightarrow x_2)\right] dx_1\, dx_2\,, \tag{27}$$

where the sum is over all partons contributing to the three subprocesses $q\bar{q} \to W^-W^+g$, $qg \to W^-W^+q$, and $\bar{q}g \to W^-W^+q$. The squared matrix elements for the $2 \to 3$ subprocesses were evaluated numerically via helicity amplitude methods as described in Ref. [9]. The integration over three-body phase space and $dx_1\, dx_2$ is done numerically by standard Monte Carlo techniques. The kinematic invariants $s_{ij}$ and $t_{ij}$ are first tested for soft and collinear singularities. If an invariant for a subprocess falls in a soft or collinear region of phase space, the contribution from that subprocess is not included in the cross section.

## IV. RESULTS

The numerical results presented in this section have been obtained using a single scale $Q^2 = M_{WW}^2$, where $M_{WW}$ is the invariant mass of the $W$ pair, for the renormalization scale $\mu^2$ and factorization scale $M^2$. The two-loop expression for $\alpha_s$ has been used. The QCD scale $\Lambda_{\rm QCD}$ is specified for four flavors of quarks by the choice of parton distribution functions and is adjusted whenever a heavy-quark threshold is crossed so that $\alpha_s$ is a continuous function of $Q^2$. The heavy-quark masses were taken to be $m_b = 5$ GeV and $m_t = 140$ GeV [20]. The standard model parameters were taken to be $M_Z = 91.17$ GeV, $M_W = 80.0$ GeV, and $\alpha(M_W) = 1/128$. These mass values are consistent with recent measurements at the Fermilab Tevatron [21], the SLAC Linear Collider [22], and the CERN $e^+e^-$ collider LEP [23]. The soft and collinear cutoff parameters were taken to be $\delta_s = 5\times10^{-2}$ and $\delta_c = 10^{-3}$. For comparison, LL predictions obtained with the two-loop running coupling for $\alpha_s$ are also given. Using the two-loop running coupling for both the LL and

TABLE I. Predicted cross sections (in pb) for $W^-W^+$ production with no cuts at various colliders and for different sets of parton distribution functions. The leading-logarithm (LL) and next-to-leading-logarithm (NLL) results are given.

| Collider | $\sqrt{s}$ (TeV) | | HMRSE | HMRSB | DFLM160 | DFLM260 | DFLM360 |
|---|---|---|---|---|---|---|---|
| Tevatron | 1.8 | LL | 7.87 | 7.44 | 7.25 | 6.79 | 6.37 |
| Tevatron | 1.8 | NLL | 9.90 | 9.53 | 9.64 | 9.17 | 8.73 |
| LHC | 16 | LL | 61.9 | 73.6 | 73.2 | 79.6 | 84.3 |
| LHC | 16 | NLL | 85.8 | 103 | 105 | 115 | 123 |
| SSC | 40 | LL | 144 | 188 | 187 | 223 | 257 |
| SSC | 40 | NLL | 212 | 278 | 277 | 335 | 388 |

NLL results provides a consistent expansion parameter so that one can judge the degree of convergence of the results. The results presented here for $W^-W^+$ production are qualitatively similar to the results for $ZZ$ production [12].

In order to get consistent NLL results it is necessary to use parton distribution functions which have been fit to next-to-leading order. The dependence of the total cross section on the choice of parton distribution functions is shown in Table I where the total cross section for $W^-W^+$ production at the Tevatron, CERN Large Hadron Collider (LHC), and Superconducting Super Collider (SSC) are given for the Diemoz-Ferroni-Longo-Martinelli [24] (DFLM) sets corresponding to $\Lambda_4 = 160$, 260, and 360 MeV and for the HMRS [25] sets B and E. The HMRS set E distributions give the extreme values, while the HMRS set B and the DFLM160 distributions yield nearly equal values. Since the DFLM260 distributions yield results that are intermediate compared to the others, they will be used in the numerical results for the remainder of this section. Note that the HMRS distributions are defined in the universal ($\overline{\text{MS}}$) scheme whereas the DFLM distributions are defined in the physical (DIS) scheme. The factorization defining parameter $\lambda$ in Eqs. (19) and (24) should thus be $\lambda = 0$ (1) for the HMRS (DFLM) distributions.

One of the motivations for performing NLL calculations is that the results often show a less dramatic dependence on the renormalization and factorization scale than the LL result. This is true for the present calculation. The $Q^2$ dependence of the total cross section is illustrated in Fig. 4 where $Q^2$ has been parametrized as $Q^2 = nM^2_{WW}$ and the total cross section is plotted versus $n$. Parts (a), (b), and (c) of Fig. 4 are for the Tevatron, LHC, and SSC, respectively. The NLL result at the Tevatron shows only a very slight decrease in scale dependence, while the NLL results at the LHC and SSC show a definite decrease in scale dependence. At the Tevatron, $W^-W^+$ production via $p\bar{p}$ interactions is dominated by valence quark interactions with average $x$ values equal to $2M_W/\sqrt{s} \approx 0.09$. For $x$ values in this range the valence-quark distributions decrease with $Q^2$. On the other hand, at the LHC and SSC the relevant $x$ ranges are smaller by factors of 9 and 22, respectively, and sea-quark interactions dominate in the $pp$ process. The sea-quark distributions show a significant increase with $Q^2$ in these $x$ regions. Thus the cross section decreases with $Q^2$ at the Tevatron but increases with $Q^2$ at the LHC and SSC. At the LHC the cross section is nearly independent of $Q^2$ because the increasing parton distributions are compensated by the decreasing of $\alpha_s$.

The NLL and LL total cross sections for $pp \to W^-W^+$

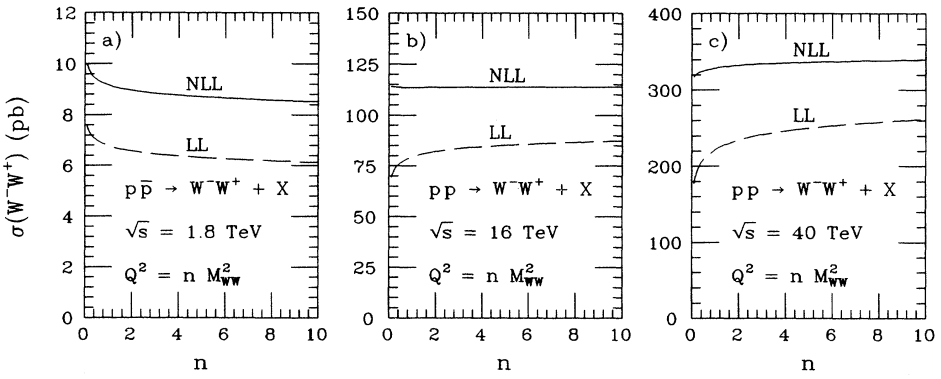


FIG. 4. Total cross section as a function of scale; the scale has been parametrized as $Q^2 = nM^2_{ZZ}$ and the total cross section is plotted versus $n$. The solid curve is the NLL result and the dashed curve is the LL result. Parts (a), (b), and (c) are for the Tevatron, LHC, and SSC center-of-mass energies, respectively.

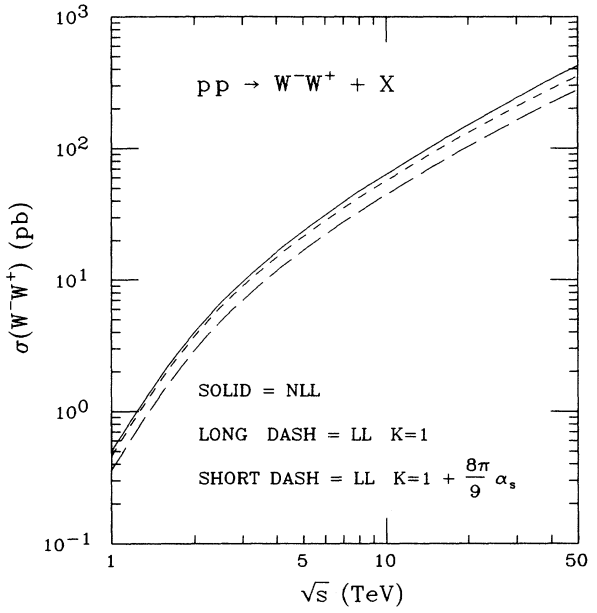


FIG. 5. Total cross section for $pp \to W^-W^+ + X$ as a function of the center-of-mass energy. The solid line is the NLL result, the long dashed line is the LL result, and the short dashed line is the LL calculation with a $K$ factor $K = 1 + (8\pi/9)\alpha_s$.

are plotted in Fig. 5 as functions of the center-of-mass energy. This figure shows that the order-$\alpha_s$ corrections are positive and increase with the center-of-mass energy. The corrections enhance the lowest-order cross section by 35–50% over the range of center-of-mass energies shown in Fig. 5. Also shown in Fig. 5 is the LL result with a multiplicative soft-gluon $K$ factor. The soft-gluon $K$ factor is an approximation for the order-$\alpha_s$ corrections and is scheme dependent. In the DIS scheme, which is used for the figures in this paper, the soft-gluon $K$ factor is $K = 1 + (8\pi/9)\alpha_s$ [10]; in the $\overline{\text{MS}}$ scheme the $\alpha_s$ term is half the size as in the DIS scheme. Figure 5 shows that the soft-gluon $K$ factor underestimates the order-$\alpha_s$ corrections; the underestimation gets worse as the center-of-mass energy increases. The underestimation is even worse in the $\overline{\text{MS}}$ scheme because the $\alpha_s$ term is only half the size as in the DIS scheme.

One of the major advantages of using Monte Carlo methods for NLL calculations is that one can calculate any number of differential distributions simultaneously by simply histogramming the quantity of interest. Figures 6, 7, and 8 show the differential distributions for the $W$-pair invariant mass $M_{WW}$, the inclusive $W$ transverse momentum $p_T(W)$, and the inclusive $W$ rapidity $y(W)$, respectively. The only cut applied to these figures is $|y(W)| < 3$. These figures show that the order-$\alpha_s$ corrections are larger at large $p_T(W)$, large $M_{WW}$, and small $y(W)$ values. Thus the corrections do not simply change the overall normalization, but instead, change the shapes of the kinematic distributions. By contrast, the soft-gluon $K$ factor simply scales up the lowest-order cross section and thus predicts no shape change in the kinematic distributions.

## V. SUMMARY

A complete next-to-leading-logarithm calculation of $p\overset{(-)}{p} \to W^-W^+$ has been presented. The calculation was done using a combination of analytic and Monte Carlo integration methods which make it easy to calculate a variety of observables and to impose experimental cuts.

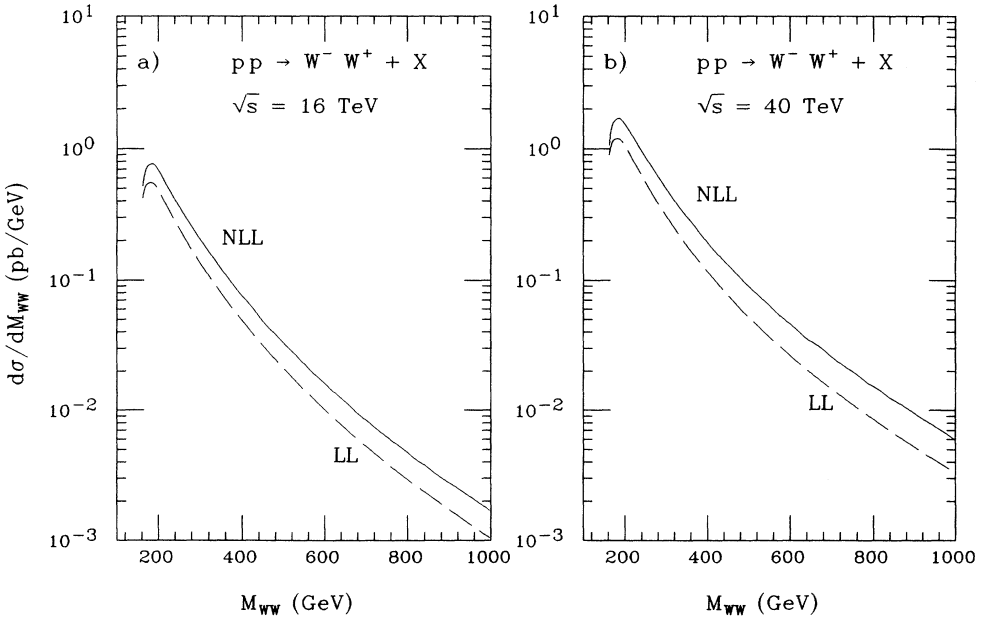


FIG. 6. Invariant mass distribution of the $W$ pair. The solid curve is the NLL result and the dashed curve is the LL result. Parts (a) and (b) are for the LHC and SSC center-of-mass energies, respectively.

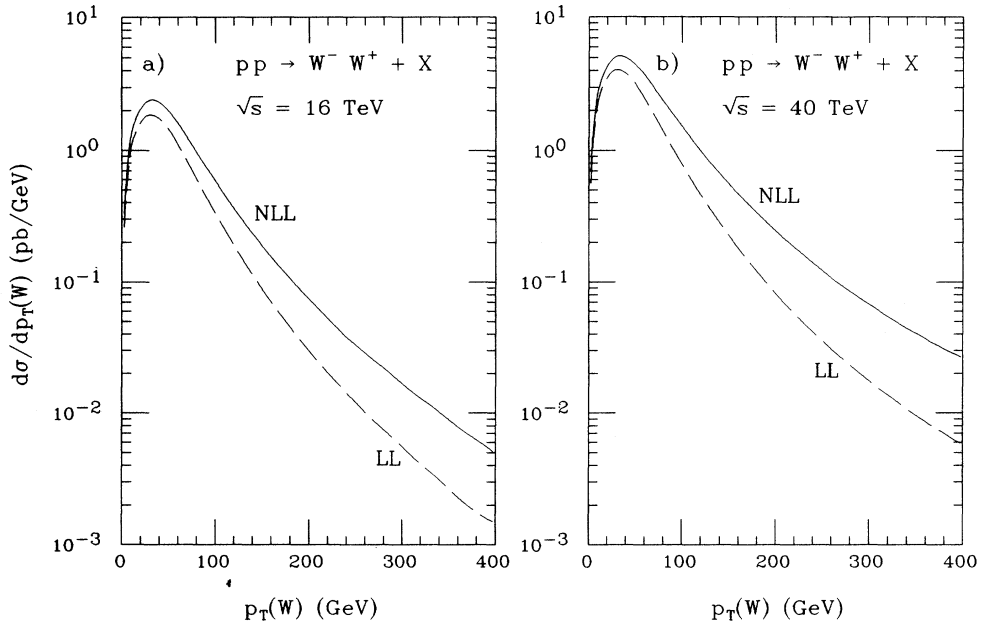


FIG. 7. Inclusive $W$-boson transverse momentum distribution. The labeling conventions are the same as Fig. 6.

The order-$\alpha_s$ corrections enhance the lowest-order cross section by 35–50%. The size of the NLL corrections depends on the observable and on the kinematic range. The NLL results are less dependent on the scale choice than the LL result, especially at supercollider energies. These results are qualitatively similar to the results for hadronic $ZZ$ production.

## ACKNOWLEDGMENTS

The author wishes to thank J. F. Owens and H. Baer for useful discussions. This research was supported in part by the U.S. Department of Energy under Contract No. DE-FG05-87-ER40319.

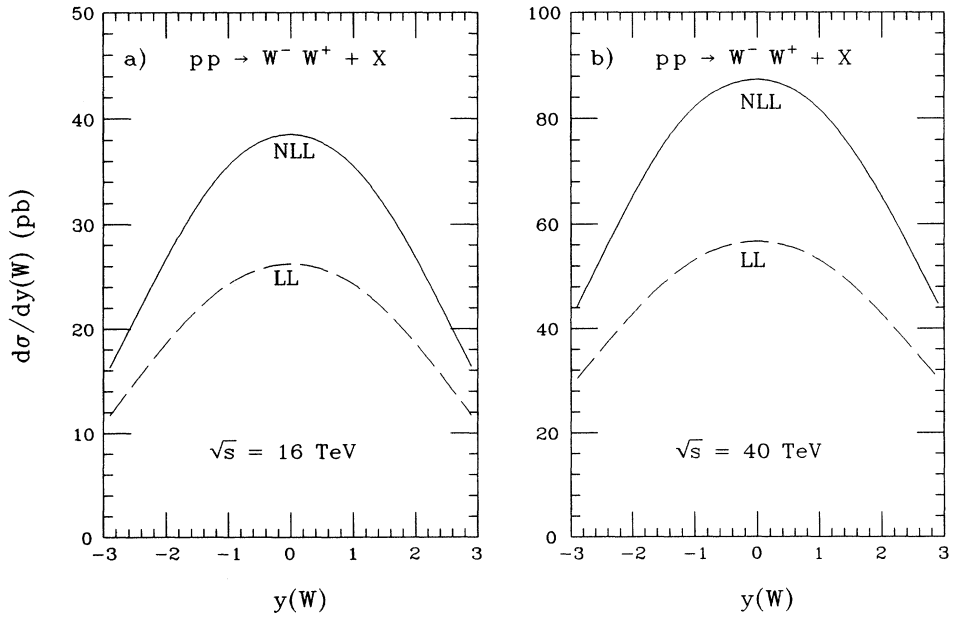


FIG. 8. Inclusive $W$-boson rapidity distribution. The labeling conventions are the same as Fig. 6.

## APPENDIX A: REGULARIZATION OF $\gamma_5$

The implementation of $\gamma_5$ in dimensional regularization requires a prescription for defining $\gamma_5$. This paper uses the definition proposed by Chanowitz *et al.* [26], who define $\gamma_5$ by the following properties: (1) $\{\gamma_5, \gamma^\mu\} = 0, \quad \mu = 0, 1, \ldots, N-1$; (2) $\gamma_5^2 = 1$, (3) $\mathrm{Tr}(\gamma_5\gamma^\mu\gamma^\nu\gamma^\omega\gamma^\tau) = 4i\epsilon^{\mu\nu\omega\tau} + O(N-4) \times$ ambiguity, when $\mu, \nu, \omega, \tau$, are in the four-dimensional subspace $\mu, \nu, \omega, \tau = 0, 1, 2, 3$. The Adler-Bell-Jackiw anomaly [27] is related to the fact that the ambiguous term cannot be explicitly defined.

The ambiguous terms are discussed in Ref. [28], where it is shown that they can be discarded. The three defining properties plus the fact that there are not enough vectors to form a nonzero contraction with $\epsilon^{\mu\nu\omega\tau}$ allow one to eliminate traces containing $\gamma_5$.

After the ambiguous terms have been discarded and the traces containing $\gamma_5$ have been eliminated, the remaining traces can be evaluated in $N$ dimensions. All $\gamma$-matrix algebra was done in $N$ dimensions and the results were checked in four dimensions. The computer algebra program FORM [18] was used to do the algebra in this paper.

## APPENDIX B: LOOP INTEGRAL

The loop integrals from the virtual graphs of Fig. 2 can be reduced to a set of 12 integrals. The first 11 integrals have been given in Ref. [12] and the twelfth integral is given in this appendix. The integral was regularized via dimensional regularization with the number of space-time dimensions set to $N = 4 - 2\epsilon$. The integral was evaluated using the Feynman parametrization technique. The twelfth integral is

$$I_{12}^{\mu\nu} \equiv \int \frac{d^N k}{(2\pi)^N} \frac{k^\mu k^\nu}{k^2 (k+p_1)^2 (k-p_2)^2}$$
$$= i\frac{F}{2s}\left[-(p_1^\mu p_1^\nu + p_2^\mu p_2^\nu)\left(2+\frac{1}{\epsilon}\right) - (p_1^\mu p_2^\nu + p_2^\mu p_1^\nu) + \frac{s}{2} g^{\mu\nu}\left(3+\frac{1}{\epsilon}\right)\right], \tag{B1}$$

where the factor $F$ is

$$F = \left(\frac{4\pi}{s}\right)^\epsilon \frac{\Gamma(1-\epsilon)}{\Gamma(1-2\epsilon)} \frac{1}{(4\pi)^2}. \tag{B2}$$

## APPENDIX C: FINITE VIRTUAL CORRECTION

The finite virtual correction for the subprocess $q\bar{q} \to W^- W^+$ is contained in the function $F^{\mathrm{virt}}(s,t,u,M_W^2)$ which can be written

$$F^{\mathrm{virt}}(s,t,u,M_W^2) = A_1^q V_1^q + A_2^q V_2^q + A_3^q V_3^q . \tag{C1}$$

The $A_i^q$ factors are defined in Eq. (7) and the $V_i^q$ are functions of the kinematic invariants. The $V_i^q$ expressions for down-type quarks are related to the $V_i^q$ expressions for up-type quarks by relations identical to Eq. (9). The type-setting of the $V_i^q$ expressions is facilitated by writing them in terms of dimensionless variables $S, T, U$ defined by

$$S = \frac{s}{M_W^2}, \quad T = \frac{t}{M_W^2}, \quad U = \frac{u}{M_W^2}, \tag{C2}$$

where $s, t, u$ are the Mandelstam variables defined in Eq. (5). The dimensionless variables are related by $S + T + U = 2$. The $V_i^q$ expressions for up-type quarks are

$$V_1^u = F_1(T,U)J_1(T,U) + F_2(T,U)\left[\pi^2 + \ln\left(\frac{S}{-U}\right)^2 - \ln(S)^2\right] + F_3(T,U)\ln(-U)$$
$$+F_4(T,U)\ln\left(\frac{S}{-U}\right) + F_5(T,U)\ln(S) + F_6(T,U)\pi^2 + F_7(T,U)J_7(S) + F_8(T,U), \tag{C3}$$

$$V_2^u = \frac{\pi^2}{3S^2}(12T^2S - 32TS - 44T^2 + 128T - 4TS^2 + 4TUS - 8S - 20TU - 64 + 2TUS^2)$$
$$+\frac{1}{S^2}(-48T^2S + 128TS + 164T^2 - 512T - 8TS^2 - 18S^2 - 16TUS + 8S + 92TU + 256 - 8TUS^2)$$
$$+T \leftrightarrow U, \tag{C4}$$

$$V_3^u = E_1(T,U)J_1(T,U) + E_2(T,U)\left[\pi^2 + \ln\left(\frac{S}{-U}\right)^2 - \log(S)^2\right] + E_3(T,U)\ln(-U)$$
$$+E_4(T,U)\ln\left(\frac{S}{-U}\right) + E_5(T,U)\log(S) + E_6(T,U)\pi^2 + E_7(T,U)J_7(S) + E_8(T,U). \tag{C5}$$

The $J_1$ and $J_7$ functions are

$$J_1(T,U) = \mathrm{Li}_2\left(\frac{1-T}{S}\right) - \mathrm{Li}_2\left(\frac{S-1}{S}\right) - \mathrm{Li}_2\left(\frac{-SU}{(S-1)(1-U)}\right) + \mathrm{Li}_2\left(\frac{-U}{S-1}\right) + \mathrm{Li}_2\left(\frac{1}{1-U}\right)$$
$$-\frac{1}{2}\ln\left(\frac{-SU}{(S-1)(1-U)}\right)^2 + \tfrac{1}{2}\ln\left(\frac{-U}{S-1}\right)^2 + \tfrac{1}{4}\ln\left(\frac{1}{1-U}\right)^2 + \tfrac{1}{4}\ln\left(\frac{1-U}{S}\right)^2$$
$$-\tfrac{1}{4}\ln\left(\frac{S}{U^2}\right)^2 + \ln\left(\frac{1-U}{S}\right)\ln\left(\frac{1-T}{-U}\right) - \tfrac{1}{2}\ln\left(\frac{1-U}{S}\right)\ln\left(\frac{S}{U^2}\right), \tag{C6}$$

$$J_7(S) = \frac{1}{x}\left[-4\mathrm{Li}_2\left(\frac{1-x}{2}\right) + 2\ln\left(\frac{1-x}{2}\right)^2 - \ln(S)^2 + \frac{\pi^2}{3}\right], \tag{C7}$$

where $x = \sqrt{1-4/S}$ and $\mathrm{Li}_2(z)$ is the dilogarithm function

$$\mathrm{Li}_2(z) = -\int_0^1 \ln(1-tz)\frac{dt}{t} = \sum_{k=1}^{\infty}\frac{z^k}{k^2}. \tag{C8}$$

The $F_i$ functions are

$$F_1 = \frac{16T}{U} - \frac{32}{U^2},$$
$$F_2 = \frac{8T}{U} - \frac{16}{U^2},$$
$$F_3 = \frac{1}{S}\left(-32 + \frac{32T^2}{U} - \frac{64T}{U} - \frac{64T}{U^2} + 48T + 16U - \frac{64}{U} + \frac{128}{U^2}\right),$$
$$F_4 = \frac{1}{(1-U)}\left(-\frac{8T}{U} + 40T + 16U - \frac{88}{U} + \frac{40}{U^2}\right), \tag{C9}$$
$$F_5 = \frac{1}{(1-U)}\left(24 - \frac{8T}{U} - 24T - 24U + \frac{48}{U} - \frac{16}{U^2}\right)$$
$$+\frac{1}{(S-4)^2}\left(-80 - \frac{8T^3}{U} + \frac{32T^2}{U} + 8T^2 + 24TU + \frac{48T}{U} - 32T + 8U^2\right),$$
$$F_6 = \frac{4}{3}\left(7 + TU - \frac{2T}{U} - 4T - 4U + \frac{8}{U^2}\right),$$
$$F_7 = \frac{1}{S(S-4)}\left(-40 - \frac{16T^2}{U} + \frac{24T}{U} + 16T + \frac{16}{U}\right) - \frac{24(U-T)^2}{SU(S-4)^2} + \frac{8T}{U},$$
$$F_8 = \frac{1}{S}\left(-144 + 16T^2U + \frac{44T^2}{U} - 40T^2 + 16TU^2 - 112TU - \frac{96T}{U}\right.$$
$$\left. -\frac{40T}{U^2} + 192T - 40U^2 + 148U - \frac{24}{U} + \frac{80}{U^2}\right) - \frac{4(U-T)^2}{U(S-4)},$$

and the $E_i$ functions are

$$E_1 = \frac{1}{S}\left(-64 - \frac{32T}{U} + 8T + 16U + \frac{80}{U}\right),$$
$$E_2 = \frac{1}{S(1-U)}\left(-72 - 4TU - \frac{16T}{U} + 20T - 8U^2 + 40U + \frac{40}{U}\right),$$
$$E_3 = \frac{1}{S}\left(32 + \frac{32T}{U} + 8T - 8U - \frac{80}{U}\right),$$
$$E_4 = \frac{1}{S(1-U)}\left(124 + 16T^2 + 12TU + \frac{8T}{U} - 84T + 16U^2 - 72U - \frac{20}{U}\right) + \frac{8US}{(1-U)^2}, \tag{C10}$$

$$E_5 = \frac{1}{S(1-U)}\left(24 + \frac{4T^2}{U} - 12T^2 + 16TU - \frac{16T}{U} + 24T + 20U^2 - 68U + \frac{8}{U}\right)$$
$$+\frac{1}{(1-U)^3}\left(20 - 4TU^2 + 4TU + \frac{4T}{U} - 4T + 12U^3 - 44U^2 + 36U - \frac{24}{U}\right) - \frac{8(U-T)}{(S-4)},$$
$$E_6 = \frac{4}{3S}\left(16 - T^2U + 4T^2 - TU^2 + 8TU + \frac{4T}{U} - 14T + 4U^2 - 13U - \frac{10}{U}\right),$$
$$E_7 = \frac{1}{S^2}(-56 - 4T^2 - 12TU + 40T - 8U^2 + 40U) - \frac{8(U-T)}{S(S-4)},$$
$$E_8 = \frac{1}{S}\left(104 + 16T^2U - 40T^2 + 16TU^2 - 80TU + \frac{88T}{U} + 100T - 40U^2 + 56U - \frac{220}{U}\right) - \frac{8S}{(1-U)}.$$


[1] E. Eichten, I. Hinchliffe, K. Lane, and C. Quigg, Rev. Mod. Phys. **56**, 579 (1984); **58**, 1065(E) (1986).

[2] B. W. Lee, C. Quigg, and H. Thacker, Phys. Rev. D **16**, 1519 (1977).

[3] C.-H. Chang and S.-C. Lee, Phys. Rev. D **37**, 101 (1988); K. Hagiwara, J. Woodside, and D. Zeppenfeld, *ibid.* **41**, 2113 (1990).

[4] R. W. Brown and K. O. Mikaelian, Phys. Rev. D **19**, 922 (1979).

[5] D. A. Dicus and C. Kao, Phys. Rev. D **43**, 1555 (1991); E. W. N. Glover and J. J. van der Bij, Phys. Lett. B **219**, 488 (1989).

[6] H. Georgi, S. L. Glashow, M. E. Machacek, and D. V. Nanopoulos, Phys. Rev. Lett. **40**, 692 (1978).

[7] M. J. Duncan, G. L. Kane, and W. W. Repko, Nucl. Phys. **B272**, 517 (1986); M. J. Duncan, Phys. Lett. B **179**, 393 (1986); A. Abbasabadi and W. W. Repko, *ibid.* **199**, 286 (1986); R. Kleiss and W. J. Stirling, *ibid.* **182**, 75 (1986); J. F. Gunion, J. Kalinowski, and A. Tofighi-Niaki, Phys. Rev. Lett. **57**, 2351 (1986); D. A. Dicus, S. L. Wilson, and R. Vega, Phys. Lett. B **192**, 231 (1987); A. Abbasabadi and W. W. Repko, Nucl. Phys. **B292**, 461 (1987); Phys. Rev. D **36**, 289 (1987); **37**, 2668 (1988); D. A. Dicus and R. Vega, *ibid.* **37**, 2474 (1988); Phys. Rev. Lett. **57**, 1110 (1986).

[8] U. Baur, E. W. N. Glover, and J. J. van der Bij, Nucl. Phys. **B318**, 106 (1989).

[9] V. Barger, T. Han, J. Ohnemus, and D. Zeppenfeld, Phys. Rev. D **41**, 2782 (1990).

[10] V. Barger, J. L. Lopez, and W. Putikka, Int. J. Mod. Phys. A **3**, 2181 (1988).

[11] A. P. Contogouris, S. Papadopoulos, and J. P. Ralston, Phys. Rev. D **25**, 1280 (1982); A. P. Contogouris and H. Tanaka, *ibid.* **33**, 1265 (1986); N. Mebarki and H. Tanaka, Mod. Phys. Lett. A **2**, 735 (1987).

[12] J. Ohnemus and J. F. Owens, Phys. Rev. D **43**, 3626 (1991).

[13] H. Baer, J. Ohnemus, and J. F. Owens, Phys. Rev. D **42**, 61 (1990); Phys. Lett. B **234**, 127 (1990).

[14] H. Baer, J. Ohnemus, and J. F. Owens, Phys. Rev. D **40**, 2844 (1989).

[15] L. Bergmann, Ph.D. dissertation, Florida State University, Report No. FSU-HEP-890215.

[16] H. Baer and M. H. Reno, Phys. Rev. **D 43**, 2892 (1991).

[17] G. 't Hooft and M. Veltman, Nucl. Phys. **B44**, 189 (1972).

[18] FORM is a computer algebra program written by J. A. M. Vermaseren (unpublished).

[19] W. L. Van Neerven, Nucl. Phys. **B268**, 453 (1986).

[20] Recent measurements of the $Z$ width and the $W$ and $Z$ masses indicate that the top-quark mass is most likely to be around 140 GeV. See, for example, U. Amaldi, A. Böhm, L. S. Durkin, P. Langacker, A. K. Mann, W. J. Marciano, A. Sirlin, and H. H. Williams, Phys. Rev. D **36**, 1385 (1987); G. Costa, J. Ellis, G. L. Fogli, D. V. Nanopoulos, and F. Zwirner, Nucl. Phys. **B297**, 244 (1988); J. Ellis and G. Fogli, Phys. Lett. B **213**, 526 (1989); V. Barger, J. Hewett, and T. Rizzo, Phys. Rev. Lett. **65**, 1313 (1990).

[21] CDF Collaboration, F. Abe *et al.*, Phys. Rev. Lett. **63**, 720 (1989).

[22] Mark II Collaboration, G. S. Abrams *et al.*, Phys. Rev. Lett. **63**, 724 (1989).

[23] ALEPH Collaboration, D. Decamp *et al.*, Phys. Lett. B **231**, 519 (1989); **235**, 399 (1990); DELPHI Collaboration, P. Aarnio *et al.*, *ibid.* **231**, 539 (1989); L3 Collaboration, B. Adeva *et al.*, *ibid.* **231**, 509 (1989); OPAL Collaboration, M. Z. Akrawy *et al.*, *ibid.* **231**, 530 (1989).

[24] M. Diemoz, F. Ferroni, E. Longo, and G. Martinelli, Z. Phys. C **39**, 21 (1988).

[25] P. N. Harriman, A. D. Martin, R. G. Roberts, and W. J. Stirling, Phys. Rev. D **42**, 798 (1990).

[26] M. Chanowitz, M. Furman, and I. Hinchliffe, Nucl. Phys. **B159**, 225 (1979).

[27] S. L. Adler, Phys. Rev. **177**, 2426 (1969); J. S. Bell and R. Jackiw, Nuovo Cimento Lett. **4**, 329 (1972).

[28] P. Aurenche and J. Lindfors, Nucl. Phys. **B185**, 274 (1981).